Halo Current and Resistive Wall Simulations of ITER

H.R. Strauss[1], Linjin Zheng[2], M. Kotschenreuther[2],W. Park[3], S. Jardin[3], J. Breslau[3], A. Pletzer[3],R. Paccagnella[4],L. Sugiyama[5],M. Chu[6], M. Chance[6], A. Turnbull[6]
[1]New York University, New York, New York,USA
[2]Institute for Fusion Studies, University of Texas, Austin, Texas 78712, USA
[3]Princeton University Plasma Physics Laboratory, Princeton, New Jersey,USA
[4]Instituto Gas Ionizzati del C.N.R., Padua, Italy
[5]MIT, Cambridge, MA,USA
[6]General Atomics, P.O. Box 85608, San Diego, California 92186, USA
strauss@cims.nyu.edu,lzheng@mail.utexas.edu

Abstract. A number of ITER relevant problems in resistive MHD concern the effects of a resistive wall: vertical displacement events (VDE), halo currents caused by disruptions, and resistive wall modes. Simulations of these events have been carried out using the M3D code [1]. We have verified the growth rate scaling of VDEs, which is proportional to the wall resistivity. Simulations have been done of disruptions caused by large inversion radius internal kink modes, as well as by nonlinear growth of resistive wall modes. Halo current flowing during the disruption has asymmetries with toroidal peaking factor up to about 3. VDEs have larger growth rates during disruption simulations, which may account for the loss of vertical feedback control during disruptions in experiments. Further simulations have been made of disruptions caused by resistive wall modes in ITER equilibria. For these modes the toroidal peaking factor is close to 1.

Resistive wall modes in ITER and reactors have also been investigated utilizing the newly developed AEGIS [2] (Adaptive EiGenfunction Independent Solution) linear full MHD code, for realistically shaped, fully toroidal equilibria. The AEGIS code uses an adaptive mesh in the radial direction which allows thin inertial layers to be accurately resolved, such as those responsible for the stabilization of resistive wall modes (RWM) by plasma rotation. Stabilization of resistive wall modes by rotation and wall thickness effects are examined.

I. Halo Current Simulations with Resistive Walls

In several resistive MHD simulational problems, the plasma model consists of three regions: the plasma core, the plasma halo region, and a resistive wall connecting the plasma to an external vacuum magnetic field.

Example problems having these regions are vertical displacement event (VDE) and halo current simulations in ITER. Another problem with some of these features is the evolution of resistive wall modes. A key problem relevant for ITER is the calculation of halo currents, which are poloidal currents penetrating the wall, parameterized by the halo current fraction F_h of the total current. The asymmetry of the halo current, parameterized by the toroidal peaking factor (TPF), is also important for calculation of stress on conducting structures. Nonlinear simulations of VDEs, disruptions, and resistive wall modes with the M3D code [1] find F_h and TPF consistent with experimental data.

M3D combines a two dimensional unstructured mesh with finite element discretization in poloidal planes [3], and fourth order finite differencing in the toroidal direction. The code is parallelized and runs on both shared and distributed memory computers.

The M3D code includes resistive wall boundary conditions, which match the solution inside the resistive wall to the exterior vacuum solution. The exterior problem is solved with a Green's function method, using the GRIN code [4]. A thin wall model is used. In the nonlinear M3D computations, the ITER first wall is taken as the resistive wall. In linear M3D computations, the first wall is infinitely resistive, and is enclosed by an outer resistive wall. The wall shapes for the linear calculations are only approximate. Realistic first and second wall shapes will be used in future work, although they will be required by GRIN to be two dimensional.

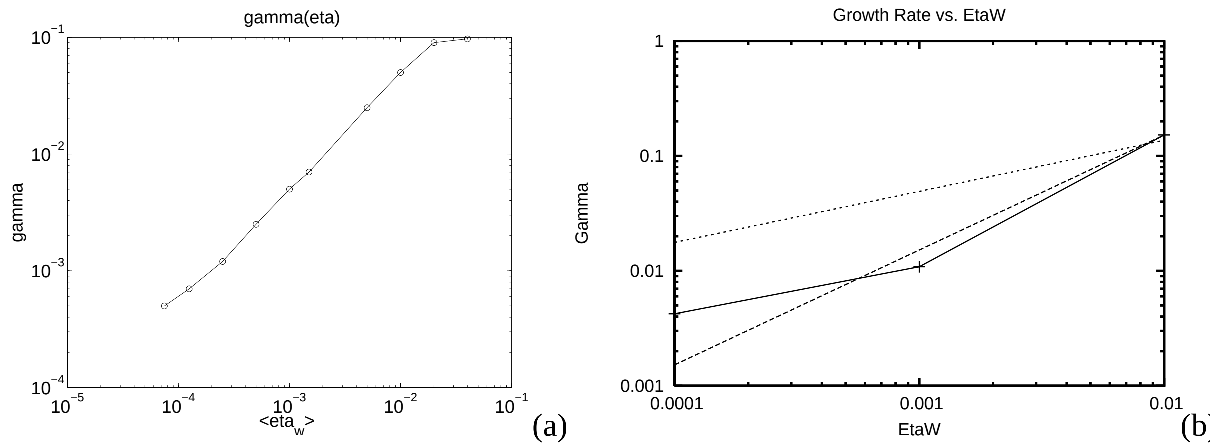

FIG. 1: *(a) scaling of VDE with η_w. (b) scaling of RWM resistive plasma mode with η_w.*

In the simulations, a self consistent resistivity proportional to the $-3/2$ power of the temperature was used. Parallel transport of temperature is treated with the "artificial sound" [1] model. In two dimensions, and in mildly three dimensional cases, the magnetic separatrix provides a temperature contrast. Open field lines are in contact with the wall, which is held at a relatively low constant temperature. In three dimensional nonlinear disruption simulations, stochastic magnetic field lines intersecting the wall cause a thermal quench.

The VDE instability growth rate is proportional to the wall resistivity η_w. This scaling is consistent with simulations, as will be shown below. To get the scaling it seems necessary to be in a regime in which the core resistive decay time τ_{core} is longer than the wall penetration time τ_w, which in turn is longer than the halo resistive decay time τ_{halo}, $\tau_{core} > \tau_w > \tau_{halo}$. Here $\tau_{core} = S\tau_A$, and $\tau_{halo} = (T_{halo}/T_{core})^{3/2}\tau_{core}$, where $\tau_A = R/v_A$ is the Alfvén time, R is the major radius, v_A is the Alfvén velocity, T_{halo}, T_{core} are temperatures in the halo and core respectively, $S = a^2 v_A/(\eta R) = 10^4$ in the simulations, where a is the geometric half width in the midplane, and S is the initial value at the magnetic axis. Fig.1(a) shows that the growth rate of the VDE scales as $\gamma \sim \eta_w/\delta_w$ in the appropriate range.

The temperature in the nonlinear stage of the VDE is shown in Fig.2(b) at time $t = 103\tau_A$, as the plasma is pulled into the divertor.

The halo current is the poloidal current flowing into the resistive wall. The normal component of the poloidal current integrated over the wall, I_h, is $I_h(\phi) = \frac{1}{2}\int |\hat{n}\cdot\mathbf{J}|Rdl$. Half the absolute value is taken in the integrand because $\nabla\cdot\mathbf{J} = 0$ implies the total normal current is zero when integrated over the wall and the toroidal angle ϕ. The toroidal peaking factor [5] is defined as the maximum of $I_h(\phi)$ divided by its toroidal average $< I_h >= 1/(2\pi)\int I_h d\phi$, that is, $TPF = I_{h(max)}/ < I_h >$. In the following simulation, $TPF \approx 2$. The ratio of halo current to total plasma current is also important. The halo current fraction F_h will be defined as the ratio $F_h =< I_h > / < I_\phi >$, where the denominator is $I_\phi = \int J_\phi dRdZ$, and the initial equilibrium value is used for I_ϕ.

The initial state has $q = 0.6$ on axis, with a $q = 1$ inversion radius including most of the core plasma. This is internal kink unstable. When the instability is sufficiently nonlinear, toroidal coupling to other modes causes a disruption. The plasma cools because of transport along stochastic field lines. This raises the resistivity and dissipates the current. This time development is seen in Fig.3(a). This is accompanied by a VDE. The toroidal peaking factor most of the time oscillates around 2. The peak value in time of $TPF = 2.8$, at which time the halo current fraction $F_h = 0.4$, as seen in Fig.3(b). The temperature is shown at the time $t = 113\tau_A$ in Fig.2(c). After the disruption and expansion to the wall, the plasma rapidly cools.

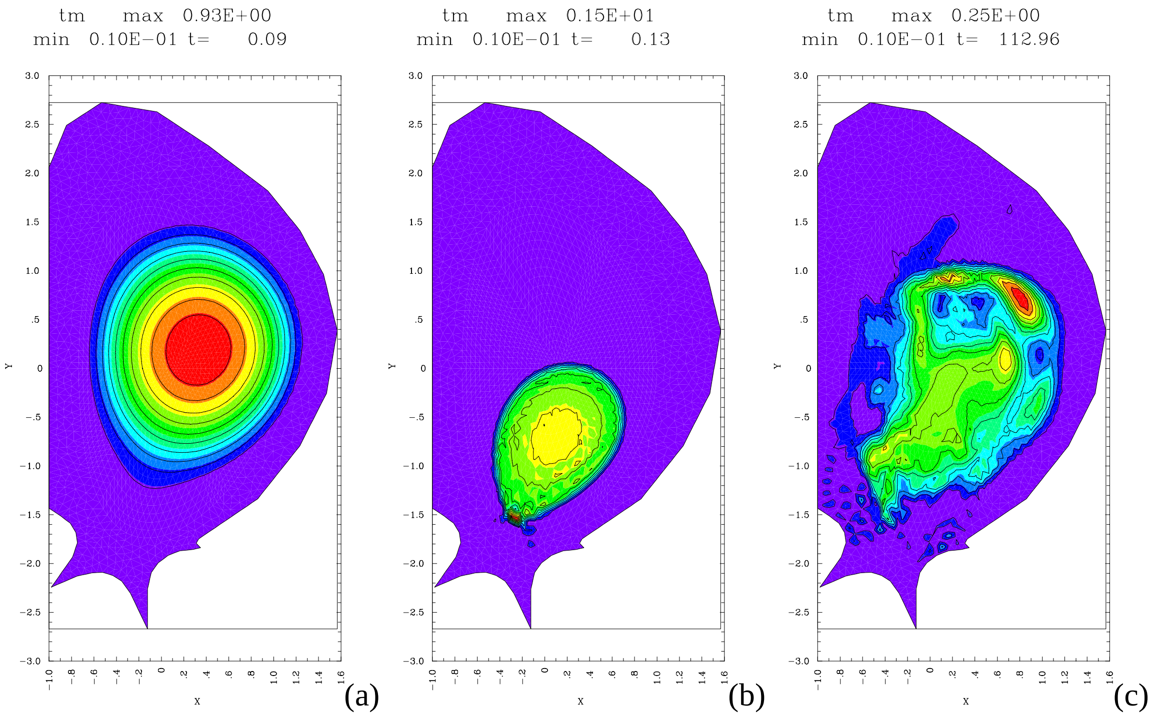

FIG. 2: *(a) temperature at t =* $0t_A$ *(b) temperature at t =* $103t_A$ *in a 2D VDE (c) temperature at t =* $113t_A$ *in a 3D disruption*

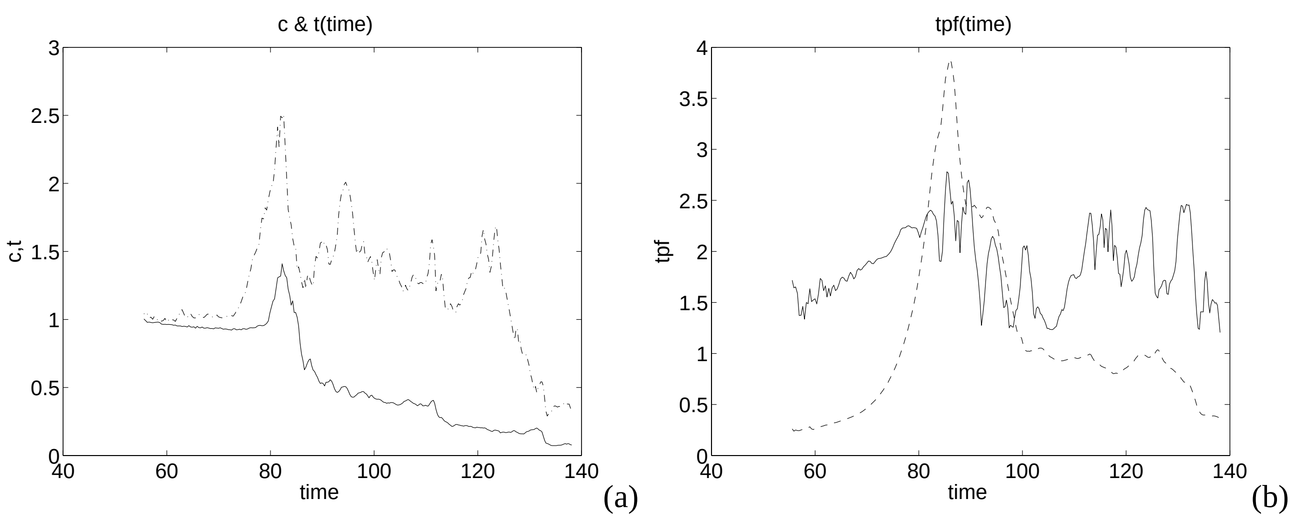

FIG. 3: *(a) normalized peak toroidal current (dotted line) and peak temperature vs. time (b) toroidal peaking factor tpf (solid line) and halo current fraction times ten,* $10F_h$, *(dashed line) vs. time*

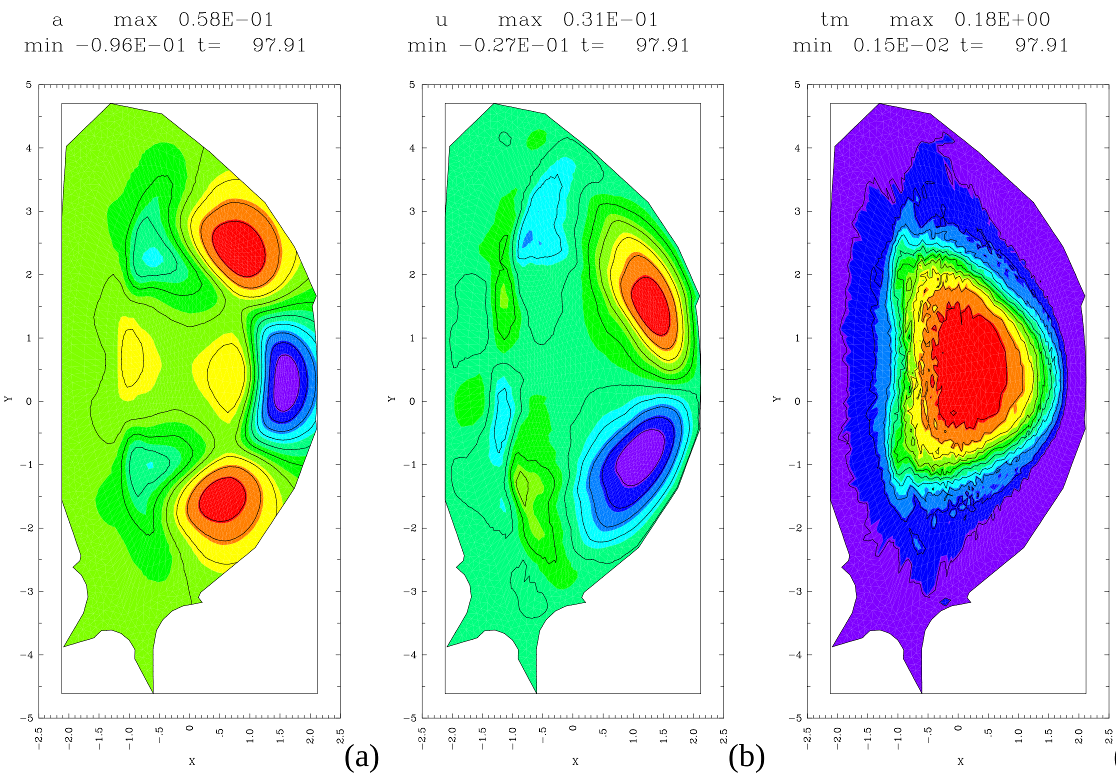

FIG. 4: *(a) perturbed poloidal magnetic flux in a resistive wall mode (b) velocity streamfunction (c) pressure*

This tends to quench halo current.

Resistive wall mode computations are complicated by the nonzero plasma resistivity and the model of the halo region as a highly resistive region. This introduces a coupling of resistive tearing and ballooning modes with resistive wall modes. If the growth rate γ_t of a tearing mode or electromagnetic resistive ballooning mode exceeds the growth rate γ_{RWM} of the resistive wall mode, the mode grows at a rate $\gamma \sim \eta^{3/5}$. When the growth rates are comparable, $\gamma \sim \eta^{1/3}\eta_w^{4/9}$ [6]. If $\gamma_{RWM} > \gamma_t$, then $\gamma \sim \eta_w$. These scalings have been verified in linear M3D simulations. Fig.1(b) shows the variation of growth rate with η_w, for dimensionless plasma resistivity $\eta = S^{-1} = 10^{-6}$, halo resistivity $= 10^{-2}$, and "vacuum" resistivity $= 1$ between the first wall and outer resistive wall. For large η_w, the growth rate scaling is linear, but at lower η_w, the scaling is $\eta_w^{4/9}$. These scalings are indicated by dashed lines. In real experiments, the resistive wall growth rate can be comparable to or less than a tearing mode growth rate, so that the modes are resistive wall resistive plasma modes.

In Fig.4 is shown a nonlinear resistive wall mode computation. The initial equilibrium is an ITER advanced tokamak case, with $q \approx 2.3$ in the plasma, with $q = 3.6$ on axis, and with $\beta_n = 2.4$. The equilibrium is unstable to free boundary external kinks. In the simulation, the first wall is resistive. Future simulations will add a second resistive wall. Fig.4(a) shows the perturbed poloidal flux function, showing flux penetration through the wall, when the mode is in a nonlinear phase of evolution. The streamfunction of the incompressible velocity component, which is approximately proportional to the electrostatic potential is shown Fig.4(b). The mode has predominant poloidal mode number 3, with toroidal mode number 1. The pressure, shown in Fig.4(c), shows the 3/1 structure. The toroidal peaking factor in this case is near 1. The peak halo current fraction $F_h = 0.2$.

II. Plasma rotation and wall thickness effects on resistive wall modes

The maximum achievable β in tokamaks is limited by the pressure driven external kink modes. The perfectly conducting wall surrounding the plasma can restrain the modes. Unfortunately, all realizable conducting walls possess non-negligible resistivity. The modes stabilized by the perfectly conducting wall are conversed to the so-called restive wall modes (RWM). Investigation of the RWM is important for improving the tokamak confinement. In this section, we address some issues for RWM in ITER that have not been completely investigated before: one is the plasma rotation effect, the other is the effect of wall thickness. For the plasma rotation effect, we consider the rotation of low Mach number in the parameter domain in which there is no perceivable particle resonance effect. The rotational stability effect in this case results from the continuum-damping-like physics. We develop a numerical formalism to deal with this fine singular layer physics. On the other hand, we note that, although considerable RWM calculations in the ITER scenario have been performed before, all of the calculations are based on the thin wall approximation. The ITER wall as was designed is actually not thin, about $0.45m$. This have motivated us to develop a theoretical formalism and code to clarify the wall thickness effect as well.

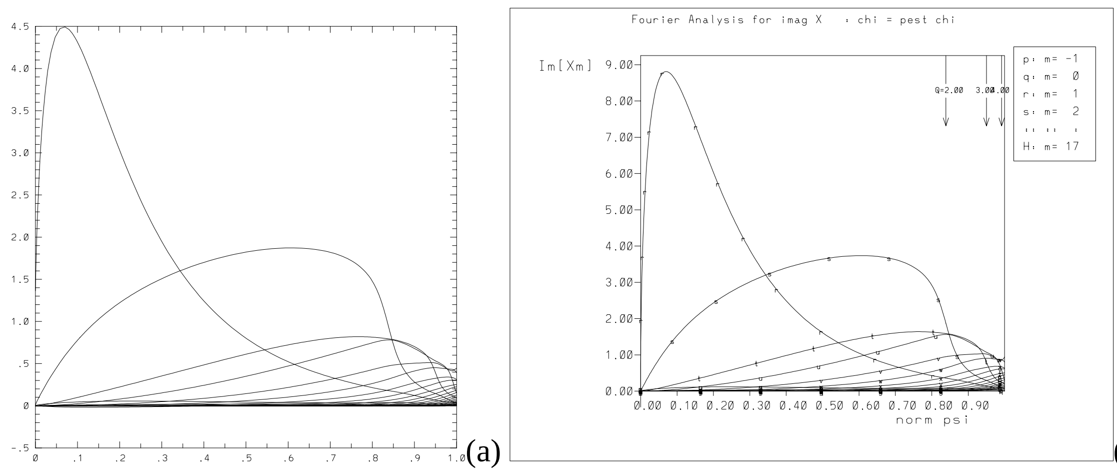

(a) (b)

FIG. 5: *n=1 mode comparison between AEGIS (a) and GATO (b).*

The investigation employs an MHD shooting code: AEGIS (Adaptive EiGenfunction Independent Solution) newly developed at the Institute for Fusion Studies, University of Texas at Austin [2].. The numerical scheme employed by AEGIS is to solve the Euler-Lagrange equations of the energy integral. A Fourier decomposition is performed in the poloidal direction. The resulting equations in the radial direction are then solved by the adaptive shooting method. Decomposition of the general solution into a linear summation of independent solutions of the Euler-Lagrange equations is employed to facilitate the adaptive shooting. A multiple region matching technique is used to overcome the numerical difficulty associated with the stiff nature of the independent solutions. Due to its adaptive feature, the AEGIS code has better resolution near the singular surfaces of the MHD modes than the nonadaptive codes. Consequently, it can be used to investigate the RWM, which is characterized by low growth rate. Comparing with other eigenvalue codes, for example PEST [7] or GATO [8], AEGIS treats matrices of smaller size: the order of number of poloidal Fourier components. While in the usual eigenvalue codes the matrix size is of the order of the product of the numbers of poloidal Fourier components and the radial grid points. This makes AEGIS be able to handle high n modes in reasonably fast computing speed due to the small memory requirement. Nyquist diagrams are built into AEGIS, as well as an eigenvalue solver. This is particularly useful in the non-ideal MHD generalization of the AEGIS code in the current phase.

To assure the correctness of AEGIS coding, extensive benchmark studies with GATO have been performed. Good agreements are observed in all aspects, such as the stability beta limit, the growth rate, the mode shape, the critical wall position, *etc.*. shows n=1 mode comparison between AEGIS and GATO for ITER like geometry.

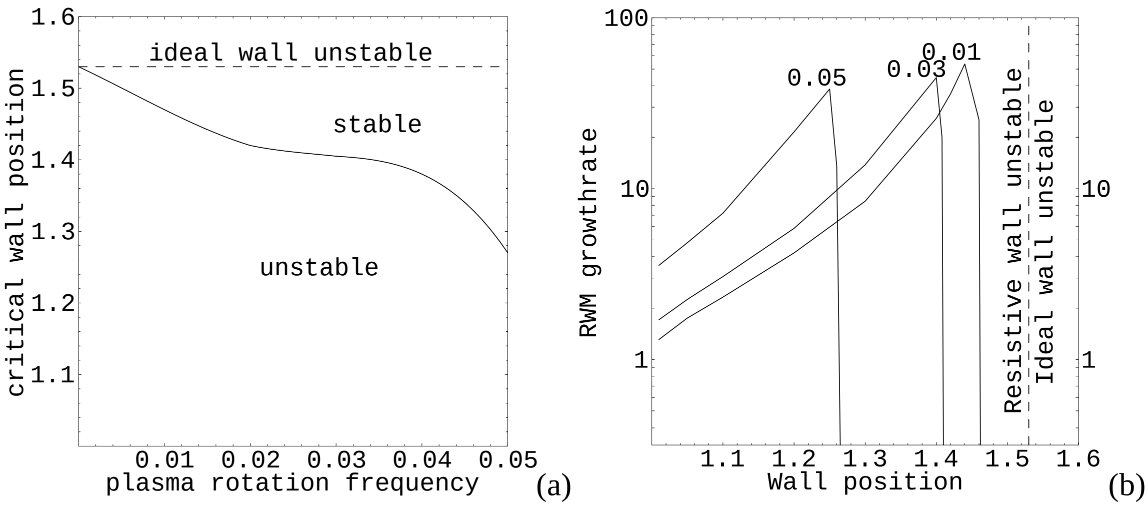

Figure 6. The rotation effect on the RWM. (a) The marginal wall position for rotation induced stability. (b) The RWM growth rate vs wall position with rotation frequency.

Various vacuum interfaces have been built in AEGIS, including the thin or thick resistive walls, the liquid metal wall, etc. The outer vacuum region (outside the wall) is calculated by the Green's function method. The inner vacuum region is, however, treated by solving the Euler-Lagrange equations using the independent solution shooting method. The shooting method is much faster than the Green's function method.

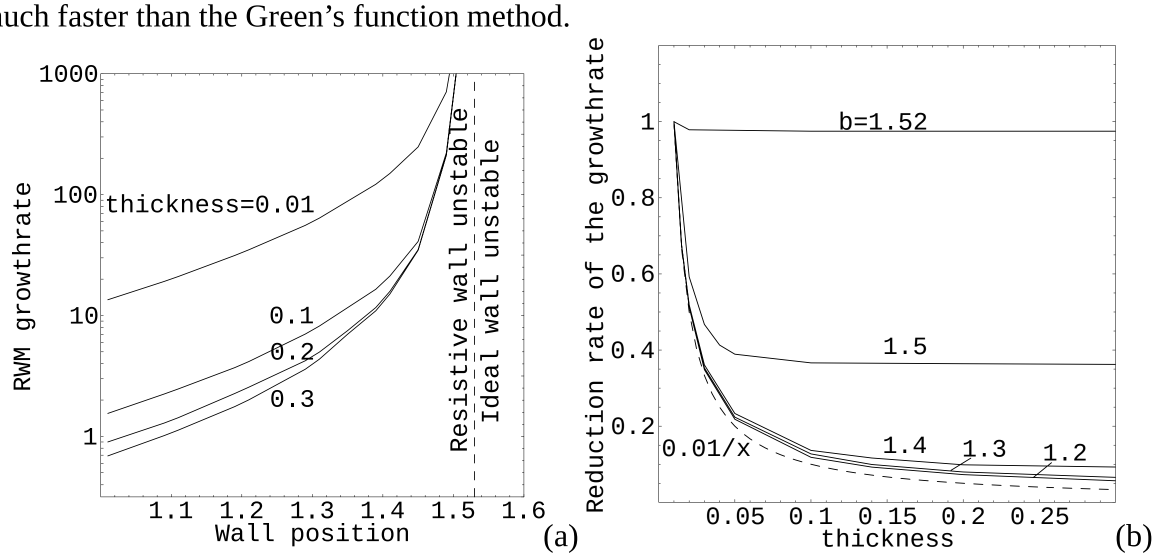

Figure 7. The wall thickness effect on the RWM. (a) The RWM growth rate vs the position of the inner side of wall with wall thickness as parameter. (b) The reduction rate of RWM growth rate vs the wall thickness with wall position as parameter The dashed curve on the right figure represents the thin wall scaling.

In the ITER design, the rotation is considered to be of low Mach number. It is lower than the ion bounce frequency, but still considerably larger than the surface averaged magnetic drift frequency. With the bounce and drift resonances being out of the parameter domain, how the rotation affects RWM in ITER needs still to be calculated. The difficulty lies in how to accurately compute the singular layer physics. With the small growth rate of the RWM the phase of the complex field line displacement variable jumps across the Alfvén continuum poles: $x \pm \Omega$, where x is the distance from the singular surface and Ω is the rotation frequency. With its adaptive feature, AEGIS can resolve the difficulty in obtaining continuum damping like effect.

The equilibrium we studied here is the ITER like, with aspect ratio being $6.2/2.00$, elongation 1.86, triangularly 0.5, $q(95) = 3$, $q(0) = 1.05$, volume average $\beta = 0.062$, and $\beta_N = 3.88$. The no wall stability limit is located at $\beta_N = 3.4$. The critical wall position is 1.53. The low Mach number rotation effect is modeled simply by replacing the complex mode frequency ω with $\omega + n\Omega$ (n the toroidal mode number). The coupling of the parallel motion, especially from the particles with small parallel velocities, is parameterized as an enhanced apparent mass effect. It is found that the plasma rotation indeed can stabilize the RWM. Typical results are summarized in Fig. 6. The calculation here is based on thin wall calculation. The coupling to the wall thickness effect is still in progress.

In dealing with the resistive wall with finite thickness, the numerical shooting based on the independent solutions of the Euler-Lagrange equations is performed. The matchings between plasma, vacuum regions, and wall at various interfaces give rise to the eigenvalue problem. In the equilibrium described previously, the wall thickness effect is summarized in Fig. 7. From Fig. 7 one can see that, although the wall thickness contributes in general a stabilizing effect in term of reducing the actual growth rate, a limit is discovered from this calculation. The part of wall located beyond the ideal-wall critical position actually does not contribute at all. This can be clearly seen from the right part of Fig. 7, especially for walls (e.g. with position 1.52 and 1.5) located near the critical wall position 1.53. The thin wall theory assumes that the reduction rate of the RWM growth rate is scaled as $1/x$. This estimate is far from the case with inner side of the wall close to the critical wall position. When the wall is brought very close to the plasma, the thin wall estimate becomes somewhat relevant.

Acknowledgment This work was supported in part by the U.S. Department of Energy. Some of the computations were performed at the NERSC supercomputer center.

References

[1] PARK, W., BELOVA, E.V., FU, G.Y., TANG, X.Z., STRAUSS, H.R., SUGIYAMA, L.E., "Plasma Simulation Studies using Multilevel Physics Models" Phys. Plasmas **6** 1796 (1999).

[2] Zheng, L.-J., Kotschenreuther, M., Turnbull, A., Waelbroeck, F., Van Dam, J. W., and Berk, H. L., Bull Am. Phys. Soc. 48, 282 (2003); L.-J. ZHENG, M. KOTSCHENREUTHER, "An adaptive ideal magnetohydrodynamics shooting code for axisymmetric plasmas", to be submitted for publication.

[3] STRAUSS, H.R., LONGCOPE, D.W., J. Comput. Phys. **147** (1998) 318.

[4] http://w3.pppl.gov/rib/repositories/NTCC/catalog/Asset/grin.html

[5] Pomphrey, N., Bialek, J., Park, W., "Modeling the toroidal asymmetry of poloidal halo currents," Nuclear Fusion 38, 449 (1998).

[6] Finn, J., Phys. Plasmas 2, 3782 (1995).

[7] R. C. GRIMM, J. M. GREENE, AND J. L. JOHNSON, "Methods of Computational Physics" (Academic Press, New York, London, 1976). Vol. 9, p. 253-280.

[8] L. C. BERNARD, F. J. HELTON, AND R. W. MOORE, Comput. Phys. Commun., 24 (1981) 377-380.